Plasmonics (2024) 19:1173–1185
https://doi.org/10.1007/s11468-023-02081-8

RESEARCH

Antibacterial Activity of Gold Nanoparticles Produced by One-Step Pulsed Laser Ablation in Liquid

Asraa B. Radhi[1] · Khawla S. Khashan[1] · Ghassan M. Sulaiman[2]

Received: 12 August 2023 / Accepted: 26 September 2023 / Published online: 30 September 2023

Abstract

In the current study, pulsed laser ablation in a liquid process was used to create gold nanoparticles (Au NPs) in the deionized distilled water. The pulsed laser ablation in liquid (PLAL) technique was used to create the NPs in two different processes. In first method, the Au nanoparticles were prepared with different laser fluences (2.2, 4.4, 6.64, 8.85, and 11.1) J.cm^{-2}, and the number of pulses was fixed at 300 pulses for each fluence. The second method uses different number of laser pulses (100, 200, 300, 400, and 500) while maintaining a consistent laser fluence (4.4 J.cm^{-2}). The characterization of nanoparticles was investigated using different techniques like UV-VIS, FTIR, XRD analysis, FE-SEM, and PL spectra. The UV-visible absorbed spectrum of Au nanoparticles revealed an absorption peak at about 530 nm and another peak at about 433 nm. The FTIR measurements have successfully shown that the entire (Au NPs), which are being generated. The X-ray diffraction pattern of the nanoparticles indicated the presence of Au nanomaterials and 111, 200, and 311 planes that correspond to Au NPs. The images of FE-SEM show that the Au NPs exhibited a spherical shape framework, agglomeration, and aggregation. With increasing laser fluence, the highest level of fluorescence emission was seen at 380 and 370 nm for Au NPs. The antibacterial activities of Au NPs were investigated using well diffusion method. Two gram-positive and two gram-negative bacteria of four different species have each been exposed to antibiotic activity. Au NPs have revealed a higher activity against tested bacteria. The results revealed that the 1250 µg/mL has high activity against *Pseudomonas aeruginosa* and *Staphylococcus aureus*, while *Streptococcus mutans* has been affected by all concentrations of Au NPs, and *Acinetobacter baumannii* has been highly affected by 1000 µg/mL and 1250 µg/mL.

Keywords Gold nanoparticles · Pulsed laser ablation in liquid · Antibacterial activity · Pathogens · Green synthesis · Nanoparticles

Introduction

In recent times, nanoparticles have emerged as a highly promising substitute for conventional materials, finding extensive applications in the domains of science and engineering. The advancement of nanotechnology necessitates the ongoing progress of alternative nanofabrication methods that align with the demands of being cost-effective, straightforward, environmentally friendly, and capable of high-throughput production. Extensive research has been conducted in the field of nanoscience on small particles (NPs) of colloidal form noble metals. Nanoparticles are commonly distinguished based on their dimensions, morphology, and heterogeneity. The initial assessment of the synthesized nanoparticles is conducted through the utilization of ultraviolet spectroscopy [1, 2]. Nanotechnology employs two primary methodologies: the "top-down" approach, in which nano-objects are fabricated from bigger objects without precise atomic-level manipulation, and the bottom-up method, also known as the reduction method, wherein nanostructures are generated by assembling atoms produced through ion reduction [3–5]. Nanoparticles can be generated through the short-pulse laser destruction of a solid target immersed in a liquid medium. Gold nanoparticles are created using a variety of techniques. A method frequently used for the creation of gold nanoparticles (Au NPs) is laser ablation. One often used method for the creation of metal nanoparticles is laser destruction in liquid. In this method,

✉ Khawla S. Khashan
khawla_salah@yahoo.com

[1] Laser Science and Technology Division, Department of Applied Sciences, University of Technology, Baghdad, Iraq

[2] Biotechnology Division, Department of Applied Sciences, University of Technology, Baghdad, Iraq

bulk metals are ablated in liquid media like water using pulsed lasers [6]. It is being used to create a wide variety of nanostructured materials with different sizes and forms using pulsed laser ablation in liquid. The intensity, wavelengths, and pulse duration of the used laser are just a few of the specific features that are directly related to them [7–10]. A portion of the laser energy is converted into a mechanical impulse by vaporization and plasma formation in the liquid. The plasma formation, when the laser beam interacts with the Au target, causes localized heating which causes the gold to ionize and vaporize, forming a plasma plume with high energy. This plasma contains extremely energetic species like ions and electrons. The vaporized atoms and ions condense to produce nanoparticles as the plasma rapidly cools upon expansion into a liquid medium [2, 6]. The rate of fabrication and the morphology of the nanoparticles prepared by pulsed laser ablation in liquid are dependent on several factors, including the laser wavelength, energy of the laser pulses, the absorption of laser energy by the liquid medium, and the duration of the ablation process [11–13]. The distinctive characteristics exhibited by Au nanoparticles (Au NPs) can be attributed to their elevated surface-to-volume ratio and the augmented atom count at their grain boundaries. Gold nanoparticles (Au NPs) exhibit distinct optical characteristics within the visible spectrum due to the occurrence of surface plasmon oscillation involving unbound electrons [14–16], which makes them suitable to apply in many application fields [17–22]. Therefore, in this study, pulsed laser ablation in liquid (PLAL) was utilized to synthesize Au nanoparticles and evaluate their antibacterial activity against several strains of microbes, such as *Pseudomonas aeruginosa*, *Staphylococcus aureus*, *Streptococcus mutans*, and *Acinetobacter baumannii.* The characterization of prepared Au NPs was investigated using XRD to determine the phase and crystal structure; SEM, to examine the morphology of nanoparticles, and the optical properties were carried out using Shimadzu spectrophotometers and photoluminescence.

Materials and Methods

Gold Nanoparticle Synthesis

A 99.99% pure gold plate was employed as the target material for laser ablation. The laser ablation of gold in deionized distilled water (D.D.W.) using a Q-switched Nd:YAG laser operating at the fundamental wavelength of 1064 nm, 9 ns, and 10 Hz, as shown in Fig. 1. In order to attain a significant level of laser flounce, the laser beam was focused by employing a positive lens with a focal length of 120 mm. The experiment was done using two procedures. In the first procedure, the laser fluence was varied from (2.2, 4.4, 6.64, 8.85, and 11.1) J/cm^2 with a constant number of laser pulses (300 pulses). In the second procedure, the number of laser pulses varied from 100, 200, 300, and 400 pulses, while the laser fluence was fixed at 4.4 J/cm^2. The laser light is directed and concentrated to form a laser spot with a diameter of approximately 2.4 mm. The target plate was affixed to the base of a baking vessel containing a volume of 3 mL of liquid.

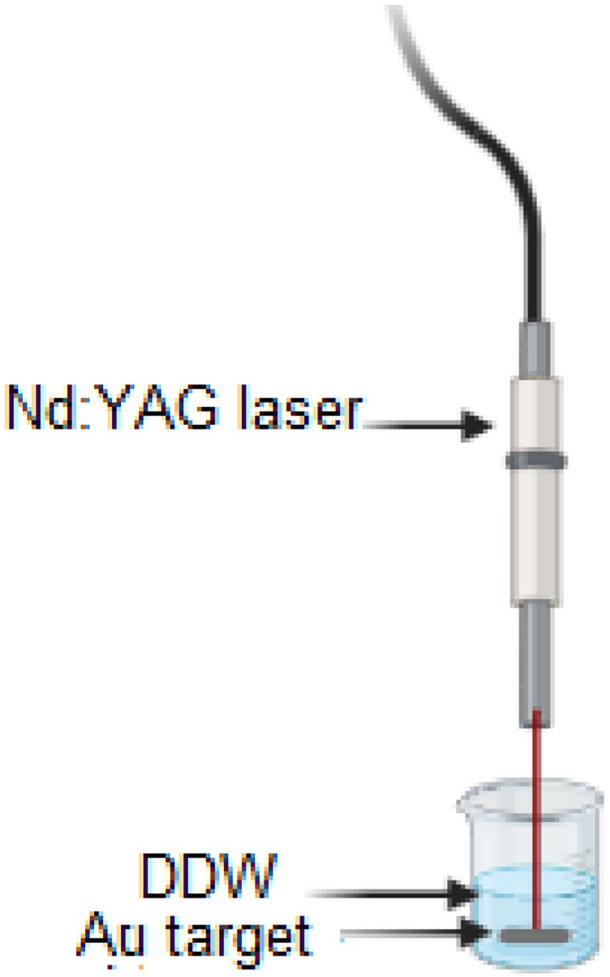

Fig. 1 Experimental setup of the PLAL

Characterization Techniques

The chemical composition of gold nanoparticles was examined using the Fourier-transform infrared spectroscopy FTIR (SPECTRUM TWO N spectrometer, PerkinElmer, Yokohama, Japan) by the KBr pellet technique in the range of 400–4000 cm^{-1}. The crystalline structure of Au NPs was characterized using an X-ray diffractometer (PODWE XRD 2700AB, Haoyuan Instrument, Dandong, China) with a

Cu K target and a tube operating at 45 kV, while the size and shape of Au NPs were examined using field emission scanning electron microscopy (FE-SEM, Czech Republic, Tescan, Mira III). Before proceeding with their examination, the samples were made by drop–casting a nanoparticle suspension on a silicon wafer. The optical properties of Au nanoparticle suspensions were carried out using a Shimadzu spectrophotometer (1900i, Shimadzu, Kyoto, Japan) in the wavelength range 300–900 nm with quartz cuvettes of 1 cm path lengths and distilled water as a blank and photoluminescence (PL) spectroscopy (G9800A, Xe lamp). These measurements were achieved using a quartzite cell with a 1-cm optical path at room temperature.

Bacterial Isolates

Various pathogenic bacteria were used: two-gram negative bacteria, *Acinetobacter baumannii* (*A. baumannii*) and *Pseudomonas aeruginosa* (*P. aeruginosa*), and two-gram positive bacteria, *Streptococcus mutans* (*S. mutans*) and *Staphylococcus aureus* (*S. aureus*). The pathogenic isolates were kindly provided from the microbiology laboratory of the Medical City Hospital, Baghdad, Iraq. Isolates were identified using the VITEK system (VITEK, Biomérieux, Marcy-l'Etoile, France) kindly supplied by the Division of Biotechnology, Department of Applied Science, University of Technology, Baghdad, Iraq.

Preparation of Mueller-Hinton Agar

Mueller-Hinton agar was prepared to reveal the antibacterial activity of Au NPs. According to the guidelines of the manufacturer, the agar was prepared by dissolving 28 g of the powder in 1000 mL of deionized distilled water with the assistance of heating and continuous shaking. After autoclaving at 121 °C for 15 min, the agar medium was cooled at 45 °C with cold water and solidified in Petri dishes which were left for about 15 min till they were cooled at room temperature.

Preparation of McFarland Solution

McFarland standard solution was prepared by adding $BaCl_2.2H_2O$ (0.05 mL, 1.175%) to H_2SO_4 (9.95 mL, 1%). The standard solution that symbolized 5×10^7 bacterial cells per milliliter was compared with turbidity bacterial suspension, which combined and made sure from its suspending. In order to mitigate the effects of evaporation, the McFarland solution was densely packed and hermetically sealed with aluminum foil to restrict the amount of light exposure.

Anti-Bacterial Efficiency Tests

The activity of Au nanoparticles against *A. baumannii*, *P. aeruginosa*, *S. mutans*, and *S. aureus* was investigated using an agar well diffusion assay. The bacteria were subcultured on brain heart infusion agar. The agar was streaked with the organisms' respective broth cultures 0.5 McFarland solution, which corresponded to the microbial concentration of 5×10^7 CFU/mL, and left for 15 min for the absorption to occur. Afterward, the end of a sterile Pasteur pipette (5 mm in diameter) was used to make wells in agar, and 70 µL of Au NPs at various concentrations (500, 750, 1000, and 1250 µg/mL) was poured into each hole. Deionized distilled water was used as a negative control. After 24 h of incubation at 37 °C, the diameters of the inhibition zones were measured in millimeters by measuring the diameter of circular inhibition zones around the well using a physical ruler.

Results and Discussion

The absorbance spectra of gold nanoparticle Au NPs synthesized by PLAL as a function of laser fluence (2.2, 4.4, 6.64, 8.85, and 11.1) J/cm^2 with 300 laser pulses are shown in Fig. 2. The peak of absorption intensity was observed at 530 nm, which increased as laser fluence increased. This indicates an increase in the concentration of Au nanoparticles. Also, the position and height of the peak in the absorption spectrum depend on the shape, size, and yield of the obtained particles. This phenomenon can be attributed to surface plasmon resonance's impacts, which are contingent upon the size and shape of the nanoparticles [23, 24]. The absorbance shows that the height of the plasmon peak increases with increasing laser fluence indicating an increase in the concentration of gold nanoparticles. This finding was substantiated by an investigation by Kuriakose et al. and Nasiri et al. [25, 26]. It was also observed that the highest degree of light absorption occurs at wavelengths of 522 and 526 nm, respectively. According to a study conducted by Prakash et al. [27], the surface of the resonance plasmon characteristic is influenced by the dimensions and morphology of the gold nanoparticles that are produced [28–30]. Figure 3 shows an absorbance spectrum of Au NPs prepared at different numbers of laser pulses (100, 200, 300, 400, and 500) and laser fluence of about 4.4 J/cm^2. The plasmon absorbance peak was shown at 433 nm and increased with an increasing number of laser pulses, indicating an increase in the concentration of gold nanoparticles.

Figures 4 displays the FTIR spectrum of gold NPs prepared with different laser fluences (2.2, 4.4, 6.64, 8.85, and 11.1) J/cm^2 and 300 pls, while Fig. 5 shows the FTIR

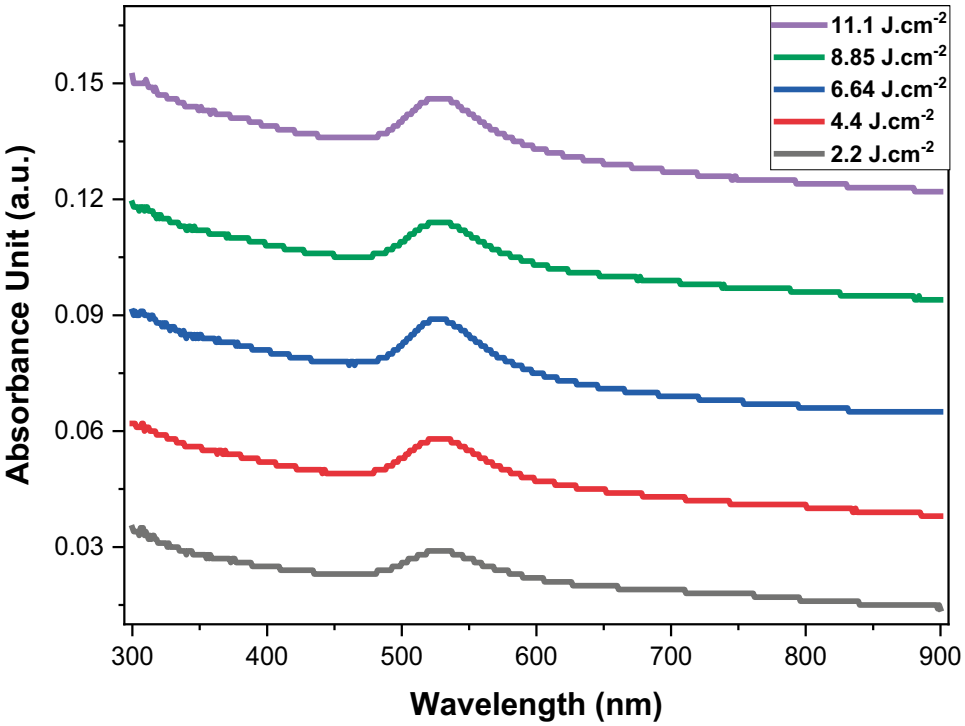

Fig. 2 UV-VIS absorbance spectra of Au NPs prepared with different laser fluence at 300 pulses

spectrum of gold NPs prepared with different numbers of laser pulses (100, 200, 300, 400, and 500) and 4.4 J/cm^2. From all FTIR spectra, the broad peaks within the range of 3200–3600 cm^{-1} are ascribed to the O–H stretching vibration, as reported in reference [31]. The peak at ~2100 cm^{-1} is identical to the stretching vibration of C=C, which is ascribed to carbon dioxide present in the atmosphere. The peak between 1630 and1660 cm^{-1} is attributed to the O–H stretching vibration mode and the bending of water. The peaks at ~710 cm^{-1} demonstrate the vibration properties of NPs. These specified functional assemblies could have been involved in reducing the metal ions, donating electrons to the

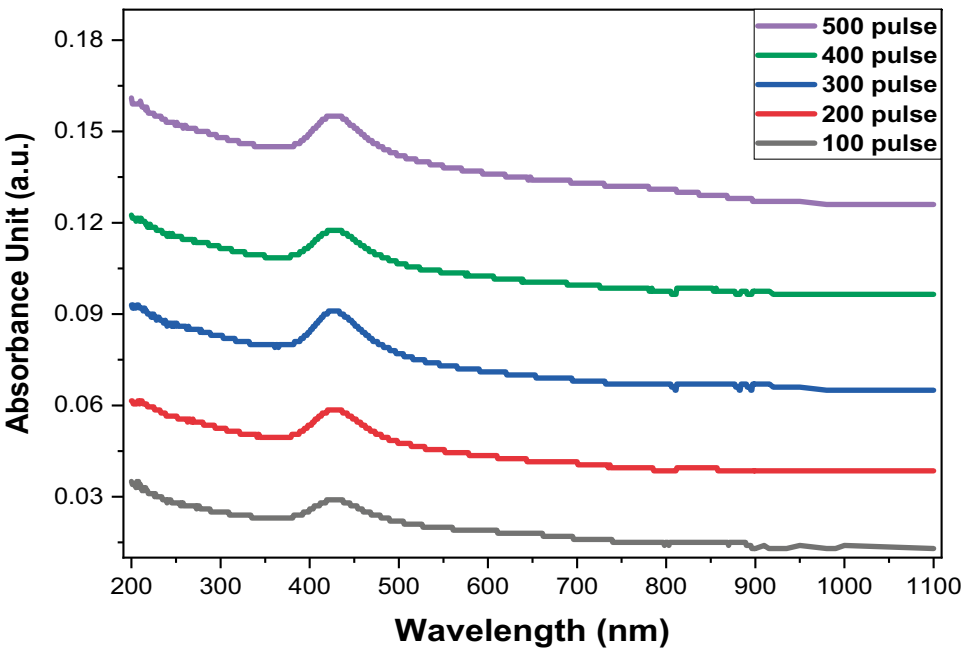

Fig. 3 UV-VIS absorbance spectra of Au NPs prepared at laser fluence 4.4 J/cm^2 with different pulses

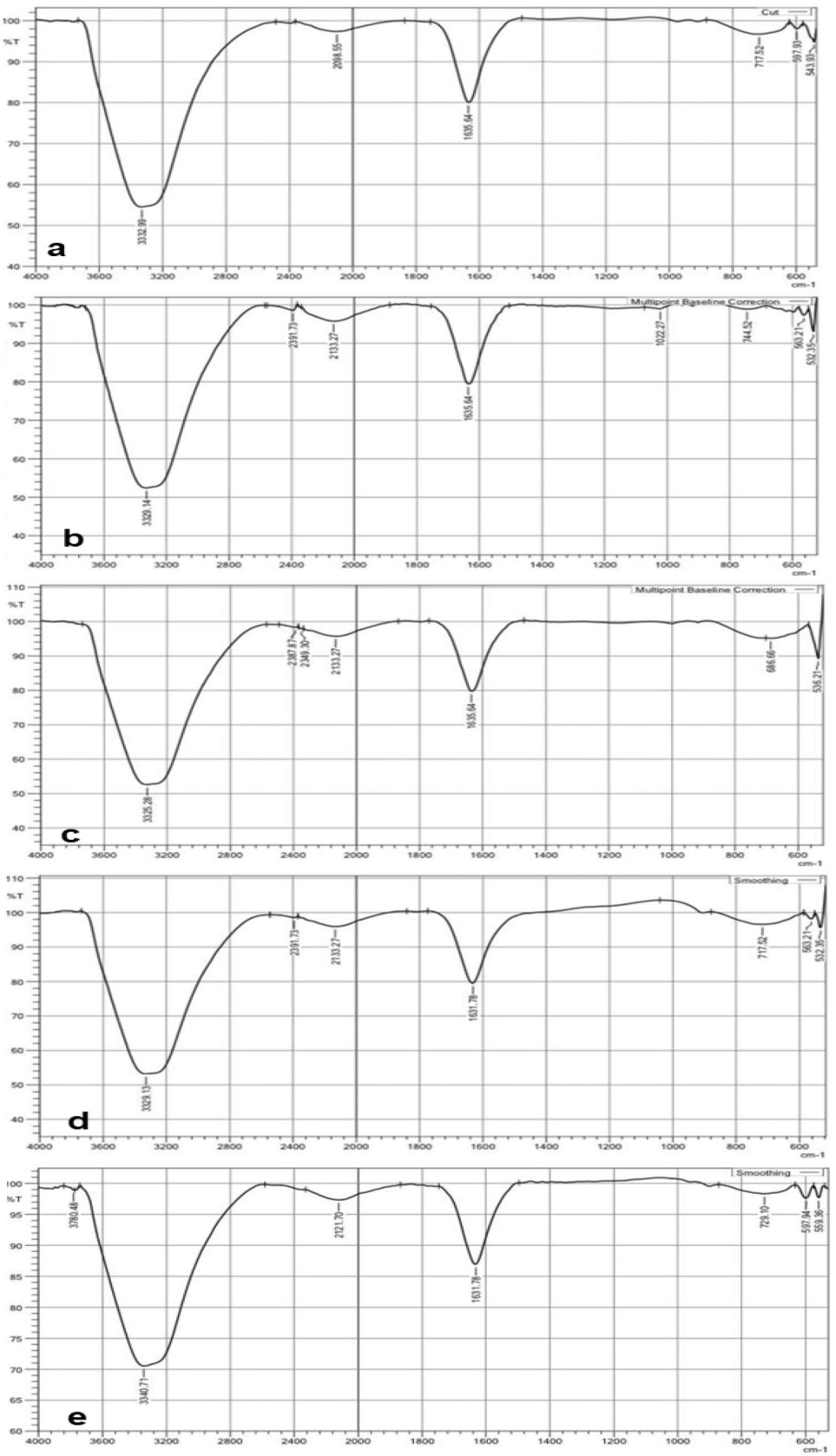

Fig. 4 FTIR spectra of Au NPs prepared with different laser fluence: **a** 2.2, **b** 4.4, **c** 6.64, **d** 8.85, and **e** 11.1 J/cm^2 and 300 pulses

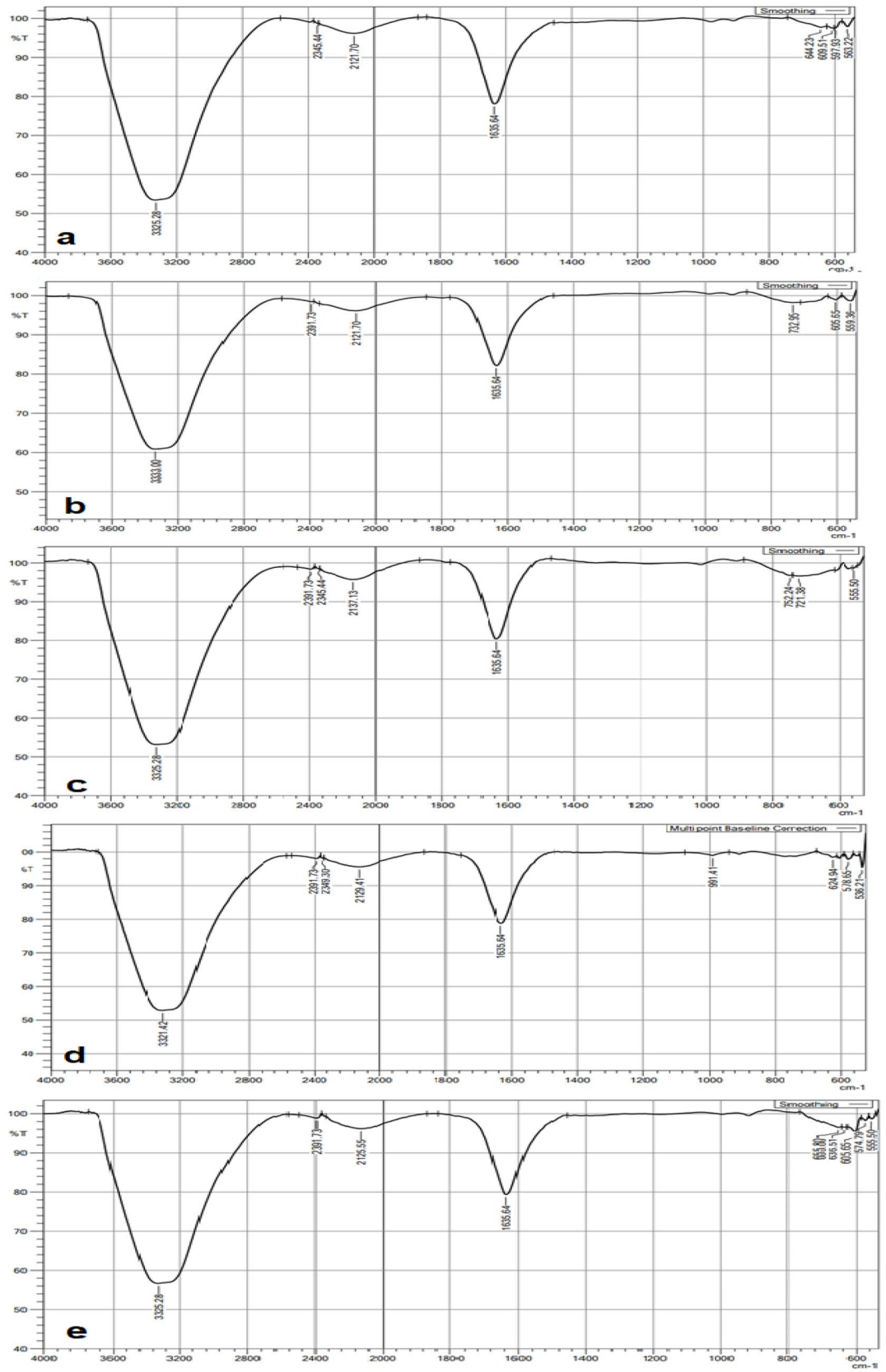

Fig. 5 FTIR spectra of Au NPs prepared at laser fluence 4.4 J/cm^2 and different number of pulses: **a** 100, **b** 200, **c** 300, **d** 400, and **e** 500 pulses

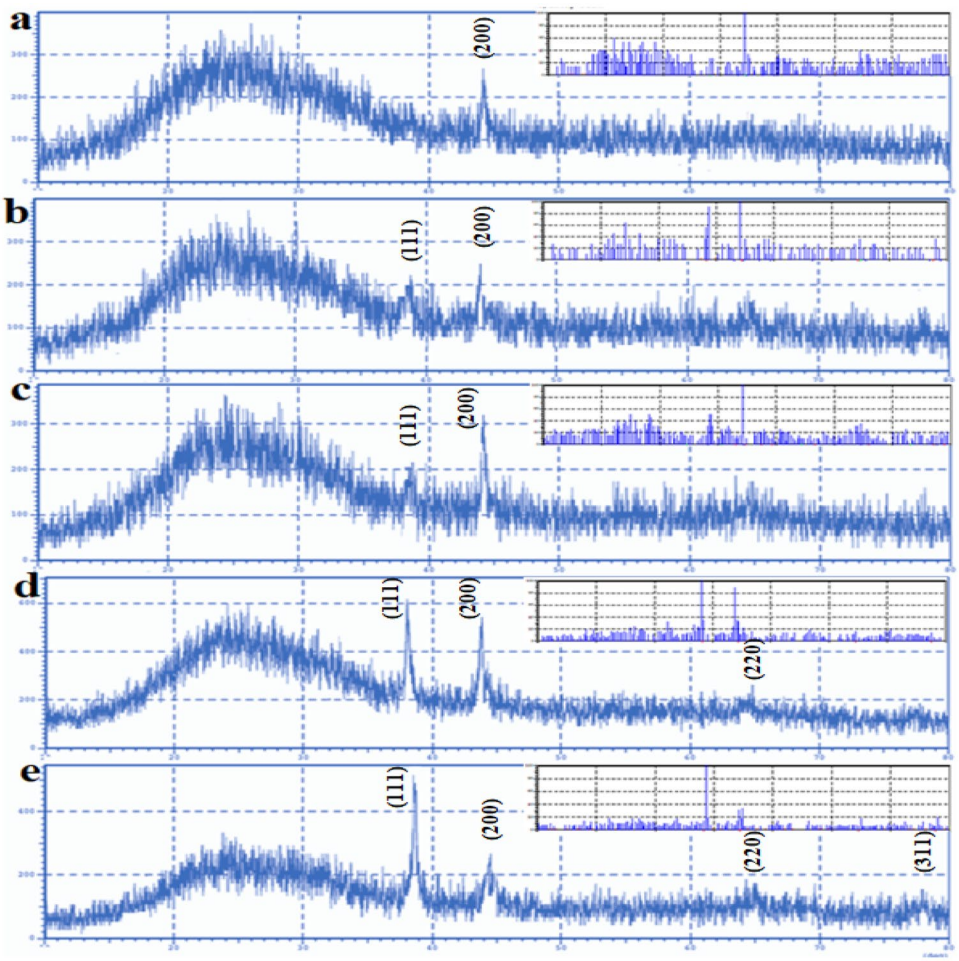

Fig. 6 XRD analysis of Au NPs prepared by PLAL in D.D.W at 300 pulses with different laser fluences: **a** 2.2, **b** 4.4, **c** 6.64, **d** 8.85, and **e** 11.1 J/cm^2

stability of NPs, and helping to avoid their agglomeration. Also, a peak about ~500 cm^{-1} is the fingerprint of Au-NPs. The confirmation of the creation of NPs of Au was established based on the results obtained from FTIR analysis. The spectral peaks exhibit a shift toward higher wavenumbers upon an increase in laser fluence, commonly referred to as a blue shift. These results are in full agreement with previously published data by Gurunathan et al. [32].

Figure 6 shows the XRD pattern in the 2θ range 10°–80° for Au NPs prepared by PLAL in D.D.W. with different

Table 1 Displays the findings of an XRD analysis of Au NPs

Laser fluence (J/cm^2)	2 theta (degree)	d-spacing (A)	I/I$_1$	FWHM (degree)	hkI planes
2.2	44.2012	2.04740	100	0.12800	200
4.4	43.7839	2.06594	89	0.32500	200
	38.0828	2.36106	100	0.28500	111
6.64	44.8408	2.01967	33	0.22000	200
	38.6389	2.32835	68	0.11200	111
8.85	43.7914	2.06560	20	0.04000	200
	38.5399	2.33411	50	0.13000	111
	64.6028	1.44150	16	0.16000	220
11.1	77.5742	1.22967	13	0.15000	311
	38.9862	2.30841	30	0.07670	111
	44.1845	2.04813	100	0.30670	200
	64.1963	1.44965	20	0.05330	220

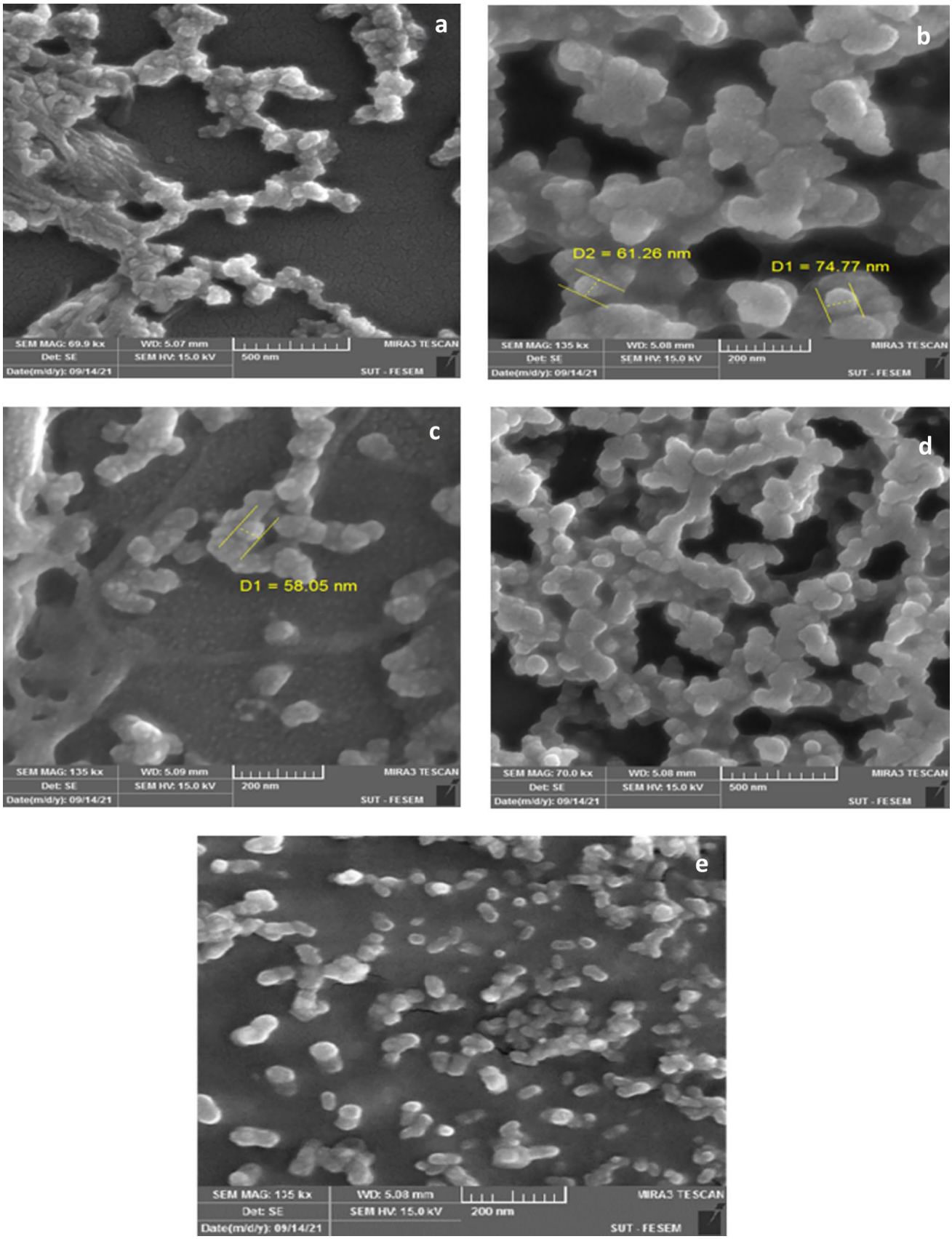

Fig. 7 FE-SEM images of Au NPs prepared by PLAL in D.D.W. with 300 pulses and different laser fluences **a** 2.2, **b** 4.4, **c** 6.64, **d** 8.85, and **e** 11.1 J/cm^2

laser fluences (2.2, 4.4, 6.64, 8.85, and 11.1) J/cm^2 and 300 pulses. Patterns exhibit peaks due to diffraction from (2θ) of ≈38.5°, 43.7°, 64.6°, and 77.5°, which return to the 111, 200, 220, and 311 reflection phases of the sample under consideration, which comprises metallic nanoparticles of gold arranged in distinct planes, as per JCPDS no. 04-0784. Based on the X-ray diffraction (XRD) pattern analysis, it can be inferred that the synthesized nanoparticles are crystalline in nature and exhibit a face-centered cubic structure, which is indicative of the presence of gold (Au) nanoparticles. The evident broadening of X-ray diffraction peaks suggests that specimens possess a nanocrystalline characteristic (Table 1) [33, 34].

Figure 7 shows the FE-SEM images of Au NPs prepared by PLAL in D.D.W. at 300 pulses with different laser fluences (2.2, 4.4, 6.64, 8.85, and 11.1) J/cm^2, and Fig. 8 shows the FE-SEM images of Au NPs prepared by PLAL in D.D.W. at laser fluence 4.4 J/cm^2 with different numbers of laser pulses (100, 200, 300, 400, and 500). This showed that the surface morphology of Au nanoparticles has an agglomerated form. The sample is made up of uniform nanoparticles of nearly spherical morphology with a narrow size distribution. This agglomeration is owing to electrostatic force among Au nanoparticles [35, 36].

The PL spectra of the nanoparticles of gold are depicted in Fig. 9. Prepared by the PLAL method, with constant pulses (300) and different laser fluences (2.2, 4.4, 6.64, 8.85, and 11.1) J/cm^2, the maximum intensity of fluorescent emission for Au NPs was obtained at a higher peak of ~380 nm. These results revealed that the increased laser

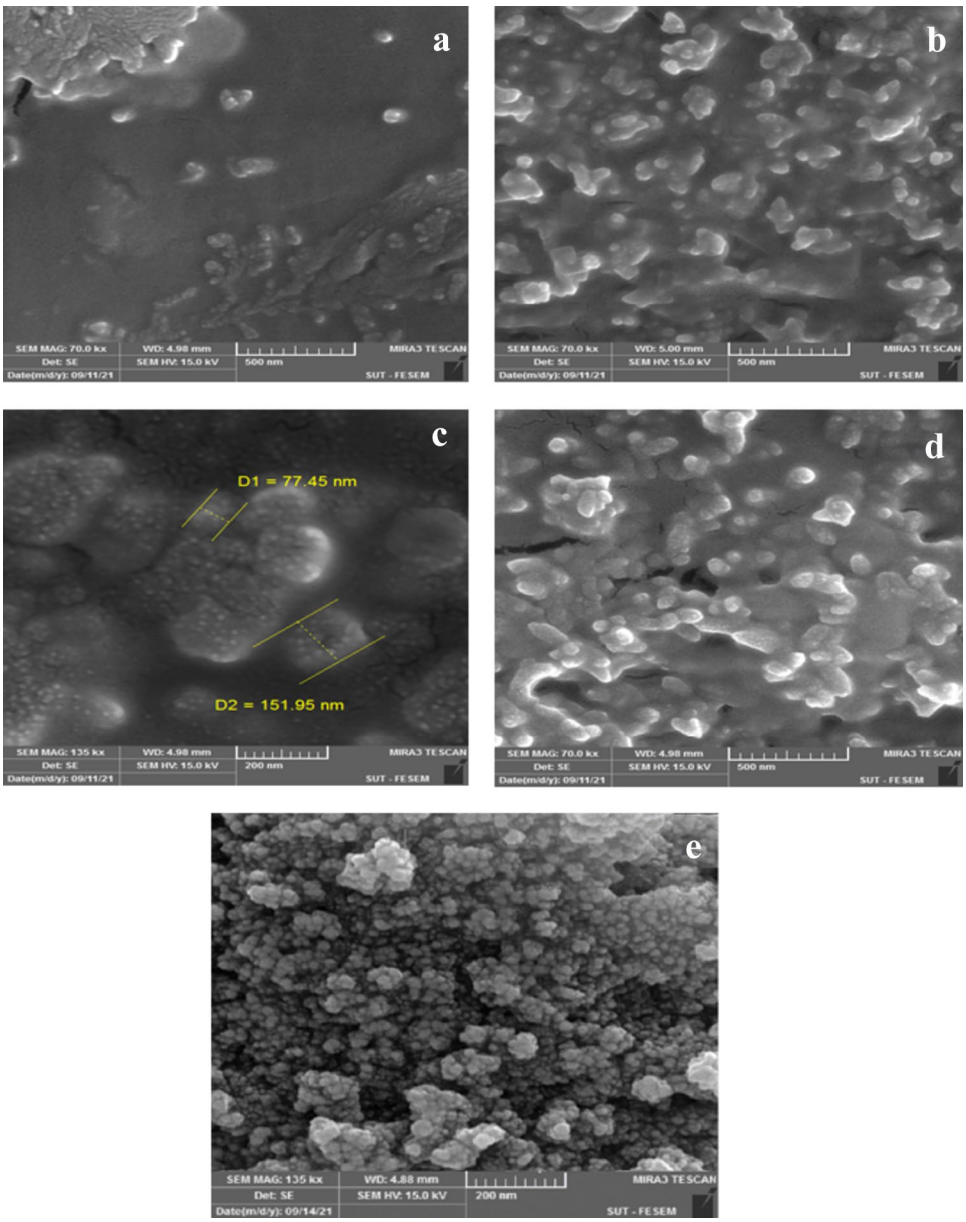

Fig. 8 FE-SEM images of Au NPs prepared by PLAL in D.D.W. with 4.4 J/cm^2 and different numbers of laser pulses (**a** 100, **b** 200, **c** 300, **d** 400, and **e** 500)

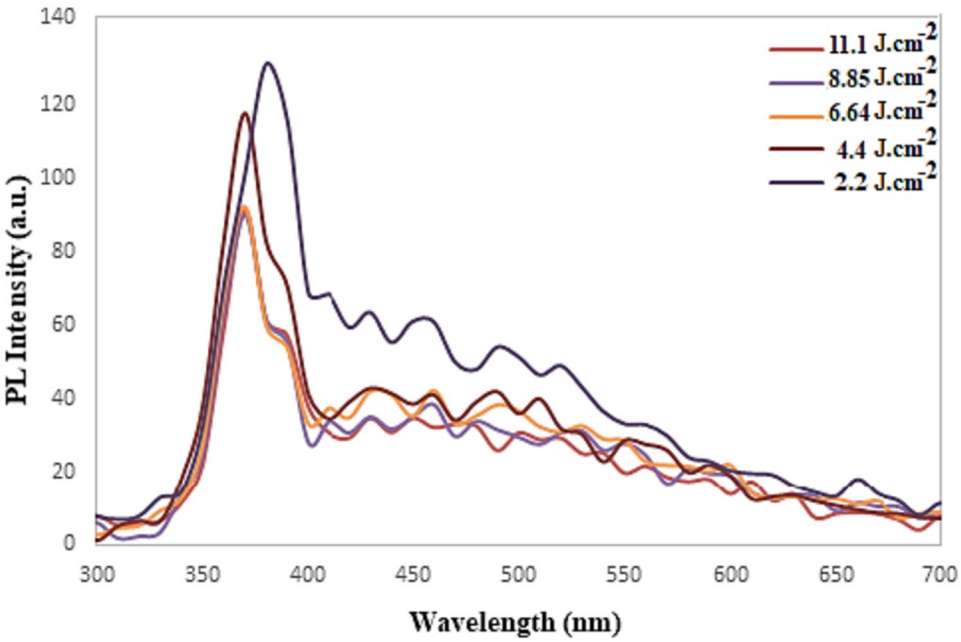

Fig. 9 Photoluminescence spectrum of Au NPs prepared by PLAL with 300 pulses and different laser fluences

fluence of AuNPs has a higher wavelength intensity. While Fig. 10 represents the PL spectra of the gold nanoparticles prepared by the PLAL method, with a 4.4 J/cm^2 laser effect and different pulses (100, 200, 300, 400, and 500) revealing the maximum intensity of fluorescent emission for Au NPs and a higher peak at ~370 nm [37–39].

Figure 11 shows the antibacterial activity of Au NPs against the four types of bacteria which included *A. baumannii*, *P. aeruginosa*, *S. mutans*, and *S. aureus* in different concentrations of Au NPs; the results revealed that the 1250 µg/mL has high activity against *Pseudomonas aeruginosa* and *S. aureus*, while *Streptococcus* has been affected by all concentrations of Au NPs; and *A. baumannii* has been highly affected by 1000 µg/mL and 1250 µg/mL [40–42]. The proposed mechanisms of the activity of the Au NPs might occur in two successive stages: firstly, by causing damage in the outer membrane of the bacterial cell wall through electrostatic or direct interaction between the cell wall and the nanoparticles. Secondly, by *production* and accumulation of *oxygen* reactive species (ROS) due to the presence of metal oxides [43]. Generation of ROS can cause changes in macromolecules such as proteins, nucleic acids, and lipids by effects of oxidative stress. These oxygen species produce free radicals that are short-lived and unstable, which influences nuclear viability and healthiness and finally leads to cell death [44, 45].

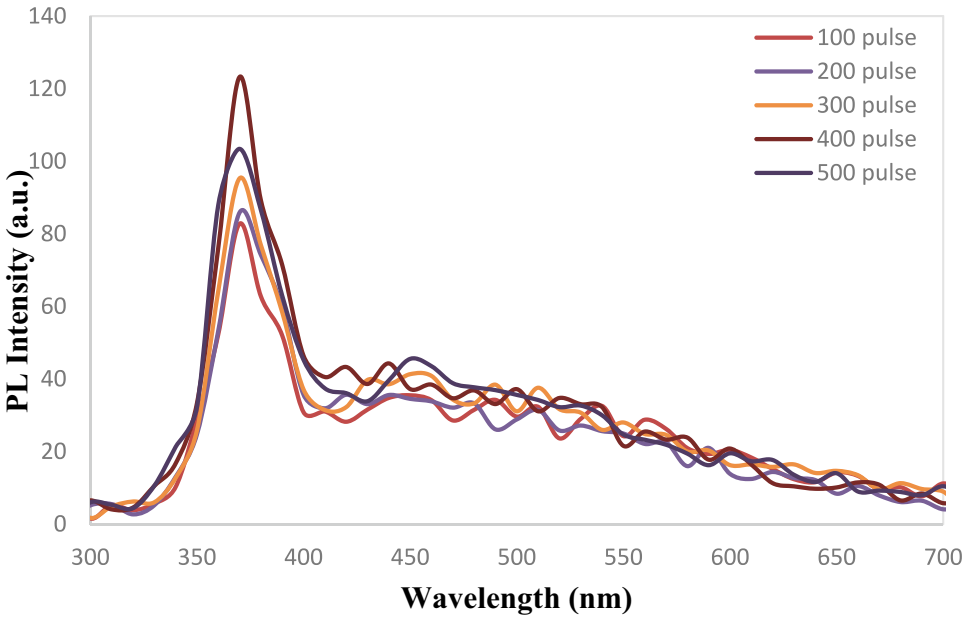

Fig. 10 Photoluminescence spectrum of Au NPs prepared by PLAL with a 4.4 J/cm^2 laser fluence and different pulses

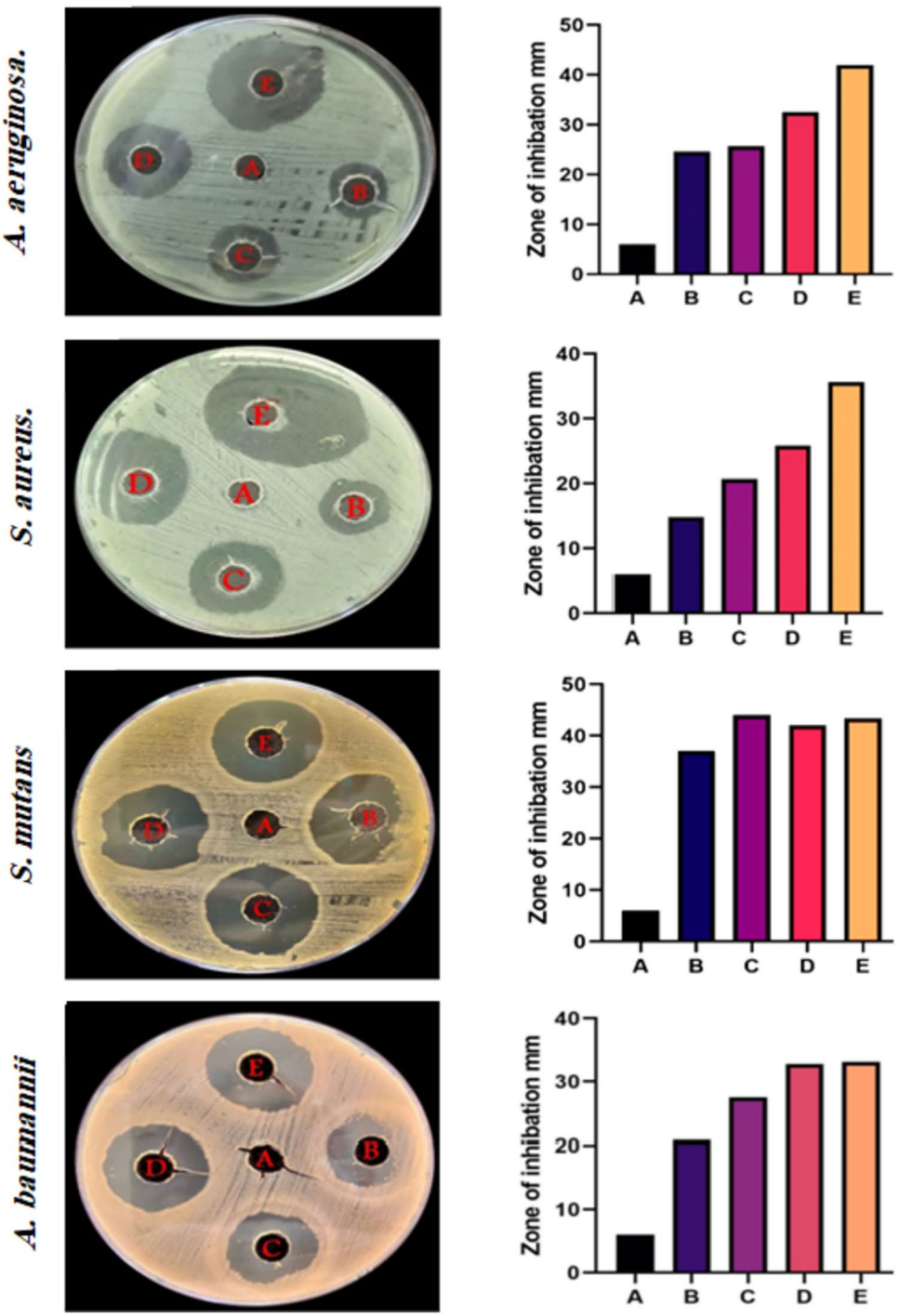

Fig. 11 Antibacterial activity of Au NPs prepared with 4.4 J/cm^2 and 500 pulses at various concentrations against *P. aeruginosa.*, *S. aureus.*, *S. mutans*, and *A. baumannii*. **A** control, **B** 500 µg/mL, **C** 750, **D** 1000 µg/mL, and **E** 1250 µg/mL

Conclusion

In this study, we investigated the successful, rapid, and easy production of Au NPs via pulsed laser ablation of gold targets in water. Fourier-transform infrared spectroscopy (FTIR), X-ray diffraction (XRD), field emission scanning electron microscopy (FE-SEM), UV-visible spectroscopy, and PL spectra were used to examine the Au nanoparticles' features. The produced nanoparticles have an almost spherical shape and high aggregation, with a face-centered cubic structure depending on the laser fluence. Eco-friendly Au NPs demonstrated potent antibacterial activity in all tested strains; this nanomaterial could be used as an alternative ingredient in antimicrobial drugs.

Acknowledgements The University of Technology in Baghdad, Iraq, provided assistance, which the authors are grateful for.

Author Contribution Conceptualization, Khawla S. Khashan, and Ghassan M. Sulaiman; methodology, Khawla S. Khashan, Ghassan M. Sulaiman, and Asraa B. Radhi; formal analysis, Khawla S. Khashan, Ghassan M. Sulaiman, and Asraa B. Radhi; investigation, Khawla S. Khashan, Ghassan M. Sulaiman, and Asraa B. Radhi; data curation, Khawla S. Khashan, Ghassan M. Sulaiman, and Asraa B. Radhi; writing—original draft preparation, Khawla S. Khashan, Ghassan M. Sulaiman, and Asraa B. Radhi; supervision, Khawla S. Khashan, and Ghassan M. Sulaiman; project administration, Khawla S. Khashan; All authors have read and agreed to the published version of the manuscript.

Availability of Data and Materials The data used to support the findings of this study are included within the article.

Declarations

Ethical Approval Not applicable.

Competing Interests The authors declare no competing interests.

References

1. Khan I, Saeed K, Khan I (2019) Nanoparticles: properties, applications and toxicities. Arab J Chem 12(7):908–931
2. Zhang J, Claverie J, Chaker M, Ma D (2017) Colloidal metal nanoparticles prepared by laser ablation and their applications. ChemPhysChem 18(9):986–1006
3. Hamad A, Li L, Liu Z (2016) Comparison of characteristics of selected metallic and metal oxide nanoparticles produced by picosecond laser ablation at 532 and 1064 nm wavelengths. Appl Phys A 122:1–15
4. Balzani V (2008) Nanoscience and nanotechnology: the bottom-up construction of molecular devices and machines. Pure Appl Chem 80(8):1631–1650
5. Khashan KS, Hassan AI, Addie AJ (2016) Characterization of CuO thin films deposition on porous silicon by spray pyrolysis. Surf Rev Lett 23(05):1650044
6. Dell'Aglio M, De Giacomo A (2020) Plasma charging effect on the nanoparticles releasing from the cavitation bubble to the solution during nanosecond pulsed laser ablation in liquid. Appl Surf Sci 515:146031
7. Hadi AA, Badr BA, Mahdi RO, Khashan KS (2020) Rapid laser fabrication of nickel oxide nanoparticles for UV detector. Optik 219:165019
8. Khashan KS, Abbas SF (2019) Indium nitride nanoparticles prepared by laser ablation in liquid. Int J Nanosci 18(02):1850021
9. Hameed R, Khashan KS, Sulaiman GM (2020) Preparation and characterization of graphene sheet prepared by laser ablation in liquid. Mater Today Proc 20:535–539
10. Khashan KS, Ismail RA, Mahdi RO (2018) Synthesis of SiC nanoparticles by SHG 532 nm Nd: YAG laser ablation of silicon in ethanol. Appl Phys A 124(6):443
11. Fadhil FA, Hasoon BA, Hussein NN, Khashan KS (2018) Preparation and characterization of CuO NPs via laser ablation under electric field and study their antibacterial activity. In: AIP Conference Proceedings, vol 2045, 1st edn. AIP Publishing
12. Khashan KS, Taha JM, Abbas SF (2017) Fabrication and properties of InN NPs/Si as a photodetector. Energy Procedia 119:656–661
13. Hasan S, Khashan KS, Hadi AA (2023) Laser-induced synthesis of palladium@ silver core–shell nps as an effective antibacterial agent. Plasmonics 18(2):689–699
14. Naharuddin NZA, Sadrolhosseini AR, Bakar MHA, Tamchek N, Mahdi MA (2020) Laser ablation synthesis of gold nanoparticles in tetrahydrofuran. Opt Mater Express 10(2):323–331
15. Sylvestre JP, Poulin S, Kabashin AV, Sacher E, Meunier M, Luong JH (2004) Surface chemistry of gold nanoparticles produced by laser ablation in aqueous media. J Phys Chem B 108(43):16864–16869
16. Qian W, Murakami M, Ichikawa Y, Che Y (2011) Highly efficient and controllable PEGylation of gold nanoparticles prepared by femtosecond laser ablation in water. J Phys Chem C 115(47):23293–23298
17. Correard F, Maximova K, Estève MA, Villard C, Roy M, Al-Kattan A, Sentis M, Gingras M, Kabashin AV, Braguer D (2014) Gold nanoparticles prepared by laser ablation in aqueous biocompatible solutions: assessment of safety and biological identity for nanomedicine applications. Int J Nanomed 5415–5430
18. Mostafa AM, Mwafy EA, Awwad NS, Ibrahium HA (2021) Au@ Ag core/shell nanoparticles prepared by laser-assisted method for optical limiting applications. J Mater Sci Mater Electron 32(11):14728–14739
19. Herrera GM, Padilla AC, Hernandez-Rivera SP (2013) Surface enhanced Raman scattering (SERS) studies of gold and silver nanoparticles prepared by laser ablation. Nanomaterials 3(1):158–172
20. Menazea AA, Ahmed MK (2020) Wound healing activity of chitosan/polyvinyl alcohol embedded by gold nanoparticles prepared by nanosecond laser ablation. J Mol Struct 1217:128401
21. Altowyan AS, Mostafa AM, Ahmed HA (2021) Effect of liquid media and laser energy on the preparation of Ag nanoparticles and their nanocomposites with Au nanoparticles via laser ablation for optoelectronic applications. Optik 241:167217
22. Priecel P, Salami HA, Padilla RH, Zhong Z, Lopez-Sanchez JA (2016) Anisotropic gold nanoparticles: preparation and applications in catalysis. Chinese J Catal 37(10):1619–1650
23. Balamurugan B, Maruyama T (2005) Evidence of an enhanced interband absorption in Au nanoparticles: size-dependent electronic structure and optical properties. Appl Phys Lett 87(14)
24. Al-Azawi MA, Bidin N (2015) Gold nanoparticles synthesized by laser ablation in deionized water. Chin J Phys 53(4):201–209
25. Kuriakose AC, Nampoori VPN, Thomas S (2019) Facile synthesis of Au/CdS core-shell nanocomposites using laser ablation technique. Mater Sci Semicond Process 101:124–130
26. Nasiri P, Doranian D, Sari AH (2019) Synthesis of Au/Si nanocomposite using laser ablation method. Opt Laser Technol 113:217–224
27. Prakash J, Kumar V, Kroon RE, Asokan K, Rigato V, Chae KH, Gautam S, Swart HC (2016) Optical and surface enhanced Raman scattering properties of Au nanoparticles embedded in and located on a carbonaceous matrix. Phys Chem Chem Phys 18(4):2468–2480
28. Mafuné F, Kohno JY, Takeda Y, Kondow T, Sawabe H (2001) Formation of gold nanoparticles by laser ablation in aqueous solution of surfactant. J Phys Chem B 105(22):5114–5120
29. Yamada K, Tokumoto Y, Nagata T, Mafuné F (2006) Mechanism of laser-induced size-reduction of gold nanoparticles as studied by nanosecond transient absorption spectroscopy. J Phys Chem B 110(24):11751–11756
30. Mafuné F, Kohno JY, Takeda Y, Kondow T (2003) Formation of gold nanonetworks and small gold nanoparticles by irradiation of intense pulsed laser onto gold nanoparticles. J Phys Chem B 107(46):12589–12596
31. Chen S, Chen A (2019) Electrochemical reduction of carbon dioxide on Au nanoparticles: an in situ FTIR study. J Phys Chem C 123(39):23898–23906
32. Gurunathan S, Han J, Park JH, Kim JH (2014) A green chemistry approach for synthesizing biocompatible gold nanoparticles. Nanoscale Res Lett 9:1–11
33. Pyrpassopoulos S, Niarchos D, Nounesis G, Boukos N, Zafiropoulou I, Tzitzios V (2007) Synthesis and self-organization of Au nanoparticles. Nanotechnology 18(48):485604

34. Lin J, Zhou W, Kumbhar A, Wiemann J, Fang J, Carpenter EE, O'connor CJ (2001) Gold-coated iron (Fe@ Au) nanoparticles: synthesis, characterization, and magnetic field-induced self-assembly. J Solid State Chem 159(1):26–31
35. Al-Omar MS, Jabir M, Karsh E, Kadhim R, Sulaiman GM, Taqi ZJ, Khashan KS, Mohammed HA, Khan RA, Mohammed SA (2021) Gold nanoparticles and graphene oxide flakes enhance cancer cells' phagocytosis through granzyme-perforin-dependent biomechanism. Nanomaterials 11(6):1382
36. Khashan KS, Badr BA, Sulaiman GM, Jabir MS, Hussain SA (2021) Antibacterial activity of zinc oxide nanostructured materials synthesis by laser ablation method. J Phys Conf Ser 1795(1):012040. IOP Publishing
37. Desarkar HS, Kumbhakar P, Mitra AK (2012) Linear optical absorption and photoluminescence emission properties of gold nanoparticles prepared by laser ablation technique. Appl Phys A 108:81–89
38. Morsi MA, Asnag GM, Rajeh A, Awwad NS (2021) Nd: YAG nanosecond laser induced growth of Au nanoparticles within CMC/PVA matrix: multifunctional nanocomposites with tunable optical and electrical properties. Compos Commun 24:100662
39. Alluhaybi HA, Ghoshal SK, Shamsuri WW, Alsobhi BO, Salim AA, Krishnan G (2019) Pulsed laser ablation in liquid assisted growth of gold nanoparticles: evaluation of structural and optical features. Nano-Struct Nano-Objects 19:100355
40. Awad MA, Eisa NE, Virk P, Hendi AA, Ortashi KM, Mahgoub AS, Elobeid MA, Eissa FZ (2019) Green synthesis of gold nanoparticles: preparation, characterization, cytotoxicity, and antibacterial activities. Mater Lett 256:126608
41. Azam A, Ahmed F, Arshi N, Chaman M, Naqvi AH (2009) One step synthesis and characterization of gold nanoparticles and their antibacterial activities against E. coli (ATCC 25922 strain). Int J Theor Appl Sci 1(2):1–4
42. Su C, Huang K, Li HH, Lu YG, Zheng DL (2020) Antibacterial properties of functionalized gold nanoparticles and their application in oral biology. J Nanomater 2020:1–13
43. Liu S, Lai Y, Zhao X, Li R, Huang F, Zheng Z, Ying M (2019) The influence of H2O2 on the antibacterial activity of ZnO. Mater Res Express 6(8):0850c6
44. Salazar L, Vallejo López MJ, Grijalva M, Castillo L, Maldonado A (2018) Biological effect of organically coated Grias neuberthii and Persea americana silver nanoparticles on HeLa and MCF-7 cancer cell lines. J Nanotechnol 2018
45. Guerrero-Florez V, Mendez-Sanchez SC, Patrón-Soberano OA, Rodríguez-González V, Blach D, Martínez F (2020) Gold nanoparticle-mediated generation of reactive oxygen species during plasmonic photothermal therapy: a comparative study for different particle sizes, shapes, and surface conjugations. J Mater Chem B 8(14):2862–2875